

Article

Catalytic Role of H₂O Molecules in Oxidation of CH₃OH in Water

Satoshi Inaba

School of International Liberal Studies, Waseda University, 1-6-1 Nishiwaseda, Shinjuku-ku, Tokyo 169-8050, Japan; satoshi.inaba@waseda.jp

Received: 22 March 2018; Accepted: 10 April 2018; Published: 12 April 2018



Abstract: We have examined the catalytic role of H₂O molecules in the oxidation of CH₃OH in water by quantum chemical simulations. A CH₃OH is decomposed into molecules, a formaldehyde and an H₂, in water, while it is converted into radicals in a gas phase reaction at a high temperature. H₂O molecules located near a CH₃OH form a first hydration shell and act as catalyst for the oxidation of CH₃OH in water. The oxidation process of a CH₃OH in water begins when a proton is delivered to a neighbor H₂O molecule from a hydroxyl of a CH₃OH. The H₂O molecule transfers an extra proton to a second H₂O molecule, a proton of which is combined with a proton detached from the methyl of the CH₃OH, forming an H₂. The energy barrier to decompose a CH₃OH is significantly reduced by the catalyst of H₂O molecules in water. A cluster of H₂O molecules arise in water as an enclosed chain of hydrogen bonds between H₂O molecules. A proton is transferred with less energy between H₂O molecules within a cluster of H₂O molecules. A cluster of five H₂O molecules further reduces the energy barrier. The calculated oxidation rate of CH₃OH with the transition state theory agrees well with that determined by experiments.

Keywords: methanol; oxidation; reaction rate; water; quantum chemical simulation

1. Introduction

Water is considered to be an ideal reaction medium to proceed chemical reactions of organic molecules efficiently when organic molecules are dissolved in water. It is possible to proceed chemical reactions to produce molecules as planned in water because the temperature and the pressure of water are controlled. Understanding chemical reactions of organic molecules in water provides us with valuable information to extract the energy of biomass without drying because biomass contains large amount of water [1]. CH₃OH is one of the simplest products by reformation of biomass and is the source of energy for a direct methanol fuel cell. It would be beneficial to study chemical reactions containing CH₃OH in water. We examine the oxidation of CH₃OH in water in this study.

The oxidation process of CH₃OH was extensively studied in the gas phase. The main channel for the oxidation of CH₃OH is identified using the detected OH absorption signals [2]. An excited CH₃OH in a shock wave or flame is primarily decomposed into two radicals as



On the other hand, it is shown that CH₃OH is decomposed into molecules in water.

Hack et al. [3] examined the oxidation of CH₃OH in a flow reactor tube made of the alloy C-276 (Ni/Mo/Cr/Fe). They used a gas chromatography and a Fourier transform infrared spectrometer and found that the major product molecules for the oxidation of CH₃OH are H₂, CO₂, and CH₄. Hydrogen gas is the most abundant product in experiments. They measured the CH₃OH concentration by a Raman spectrometer as a function of time and determined the oxidation rate of CH₃OH in water

as 1.3×10^{-2} /s at 653 K. The oxidation rate is dependent on the surface condition of the reactor, the heavy metals of which influence the oxidation rate of CH_3OH [4]. Oxygen supply into a reactor is also shown to accelerate the oxidation of CH_3OH [5].

It is interesting to investigate the effect of a reactor wall on the oxidation rate of CH_3OH . Hirsh and Franck [6] determined the oxidation rate of CH_3OH in a Ni alloy reactor with the larger volume than that used by Hack et al. They discovered the slower oxidation rate of CH_3OH due to a smaller surface to volume ratio. DiLeo and Savage [1] adopted a sealed quartz tube to perform experiments for the oxidation of CH_3OH in water without any catalyst as well as with catalyst of a Ni wire. This is the first experiment to measure the oxidation rate of CH_3OH without catalyst. They determined the oxidation rate of CH_3OH as 4.0×10^{-5} /s at 823 K, which is much slower than that given by Hack et al. (2005) in spite of the high temperature. They also found that the oxidation of CH_3OH is significantly accelerated by adding a Ni metal wire in the experiment. The catalytic effect of a Ni wire becomes weak after multiple uses in the experiments.

In our previous study, we revealed the catalytic role of H_2O molecules in chemical reactions in water by performing a number of quantum chemical simulations [7–10]. For example, H_2O molecules get involved in the dehydration process of methanediol when a proton is carried from a hydroxyl of a methanediol to an oxygen atom of the other hydroxyl to form an H_2O molecule and a formaldehyde. An H_2O molecule assists the transfer of a proton with little change of the structure of a methanediol, reducing the energy barrier for the dehydration. The calculated dehydration rate of a methanediol in water was shown to agree with that determined by experimental studies. We apply the same method to the oxidation of CH_3OH .

In the present study, we examine the catalytic role of H_2O molecules in the oxidation of CH_3OH in water by performing quantum chemical simulations. We include H_2O molecules to catalyze the oxidation in a simulation and calculate the energy barrier for the oxidation of a CH_3OH as a function of the number of H_2O molecules. H_2O molecules have hydrogen bonds with neighbor H_2O molecules and form a cluster of H_2O molecules. We include a cluster of H_2O molecules in the present simulation because we showed that a cluster of H_2O molecules becomes an active catalyst in water [7,8,10]. The effect of metal on the oxidation of CH_3OH is not considered at the present study even though it is essential when we consider the oxidation of CH_3OH in a metal reactor [11]. We calculate the oxidation rate of CH_3OH and compare it with that determined by experiments.

2. Results and Discussion

First, we optimize a tentative structure of a molecule using the B3LYP [12–14] functional with the 6-311+G(3df, 2p) basis set [15–18]. Then, we use the Gaussian 4 method to determine the optimized structure of the molecule. We examine the molecular oxidation process of a CH_3OH into an HCHO and an H_2 . The optimized structures of a CH_3OH , an HCHO , and an H_2 are displayed in Figure 1 using the MOLDEN software [19]. The bond lengths and the angle of bonds calculated with the present simulations are compared with that determined by the experimental studies [20–22]. One of the CH bond in a CH_3OH is shorter than the others because a hydrogen atom of the hydroxyl faces in the opposite direction with respect to the CH bond. We find the excellent agreement between the simulations and the experiments and confirm the Gaussian 4 method.

We locate a transition state by applying the synchronous transit guided quasi Newton method. The combinations of the H–O–C bend with the OH stretches brings a proton of the hydroxyl toward the carbon atom of a CH_3OH . Figure 2 shows a transition state for the oxidation of the CH_3OH . A bond is formed between the proton and the carbon atom, while another proton of the methyl is liberated. We find a single imaginary frequency of vibration in a transition state and confirm the discovered transition state. We execute the IRC calculation to trail the minimum energy pathway and discover local lowest energy points, which correspond to a CH_3OH and a product compound. The product compound consists of an HCHO and an H_2 .

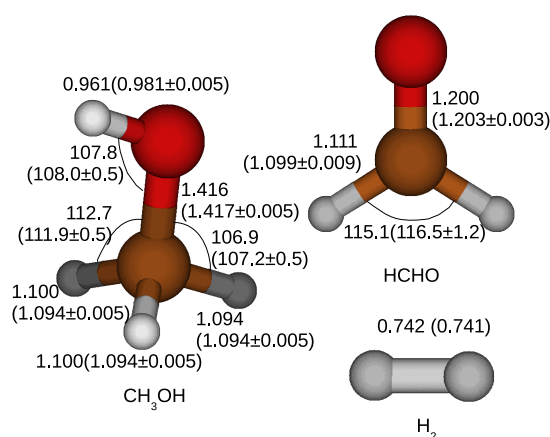


Figure 1. Optimized structures of a CH_3OH , an HCHO , and an H_2 . Red, Gray, and brown solid circles correspond to an oxygen atom, a hydrogen atom, and a carbon atom, respectively. Atoms are chemically connected with one another with a bond. The number next to a bond is the calculated bond length in the unit of \AA with that determined by an experiment [20–22] in a parenthesis.

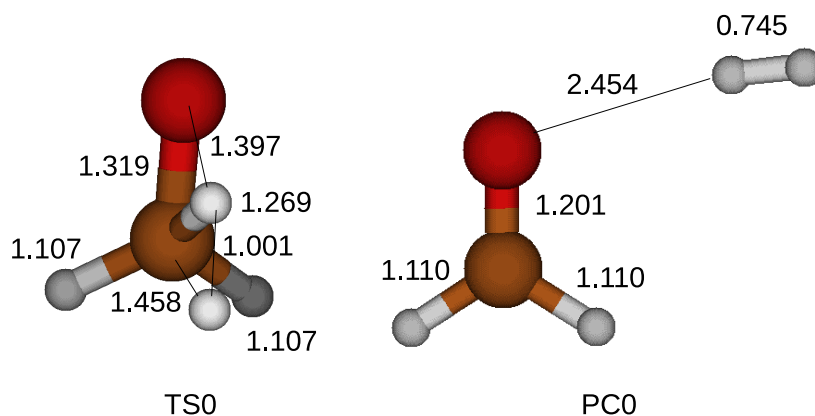


Figure 2. Optimized structure of a transition state for the oxidation of a CH_3OH without catalyst of H_2O molecules. Thin solid lines are added in the transition state to present the lengths between atoms in \AA . A product compound is displayed as well. TS0 and PC0 stand for a transition state and a product compound for the oxidation of a CH_3OH without any catalyst.

It was shown that the decomposition of formic acid and methanediol is efficiently accelerated by H_2O molecules [7–9]. H_2O molecules need to be incorporated in the simulations for the oxidation of CH_3OH in water. We use the Amber 16 [12] and find the number density distribution of H_2O molecules as a function of the distance from a CH_3OH . We carry out a molecular dynamical simulation of a CH_3OH and 2689 H_2O molecules distributed in a box (46.9 \AA , 47.7 \AA , and 48.3 \AA) for 100 pico seconds. The pressure and the temperature are controlled to keep constant values of 1 atm and 300 K.

The radial number density distribution of H_2O molecules is shown in Figure 3 as a function of the distance from the carbon atom of the CH_3OH . We normalize the number density of the H_2O molecules by the background number density of H_2O molecules. A CH_3OH expels adjacent H_2O molecules and forms an empty space with the radius of 2.8 \AA around the CH_3OH . The normalized number density of H_2O molecules increases rapidly with the increasing distance from the CH_3OH and has a maximum at 3.6 \AA , which is a first hydration shell of the CH_3OH . Beyond the first hydration shell, the normalized number density of the H_2O molecules decreases and converges to one as the distance from the CH_3OH increases because H_2O molecules distant from a CH_3OH are not influenced by the CH_3OH .

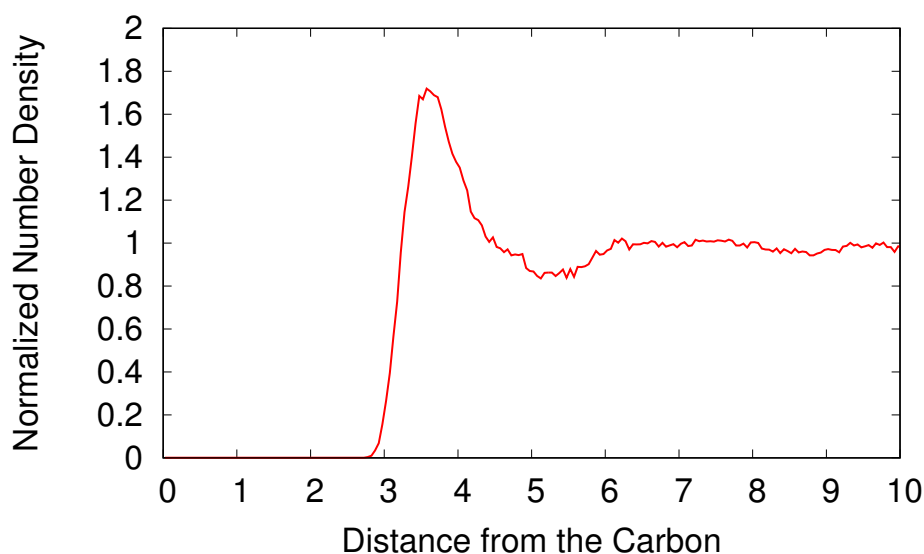


Figure 3. The normalized number density of H₂O molecules as a function of the distance from the carbon atom of a CH₃OH in Å. The number density of H₂O molecules is normalized by the background number density of H₂O molecules.

The oxidation of CH₃OH proceeds efficiently in water with the help of H₂O molecules located near a CH₃OH. The enhanced number density of H₂O molecules at the first hydration shell of a CH₃OH suggests the active catalytic role of H₂O molecules in the oxidation of a CH₃OH. We showed that H₂O molecules assist the decomposition processes of formic acid and methanediol as catalyst [7,8]. H₂O molecules are required to be included in a quantum chemical simulation to describe the oxidation process of a CH₃OH in water. We consider two structures of a supermolecule in the present study: (1) a CH₃OH and H₂O molecules form a ring structure and (2) a CH₃OH and a cluster of H₂O molecules are bonded with hydrogen bonds.

In the first structure a CH₃OH and H₂O molecules are attracted by hydrogen bonds and form a ring structure in a transition state. The optimized structures of the transition states for the oxidation of a CH₃OH are shown in Figure 4 when up to four H₂O molecules are included in the simulations. A transition state cannot be located when five H₂O molecules are introduced in a simulation.

The oxidation process of a CH₃OH starts when a proton of a hydroxyl of a CH₃OH is shared with a first neighbor H₂O molecule with the label A. The shared proton is completely transferred to the first H₂O molecule with the label A after another proton of the first H₂O molecule with the label A is shared with a second H₂O molecule with the label B when a CH₃OH and two H₂O molecules form a ring structure. On the other hand, a proton cannot be transferred to a second H₂O molecule with the label B when more than three H₂O molecules are included in the simulations. A transition state is formed when a proton is detached from the CH bond of the CH₃OH as shown in Figure 4.

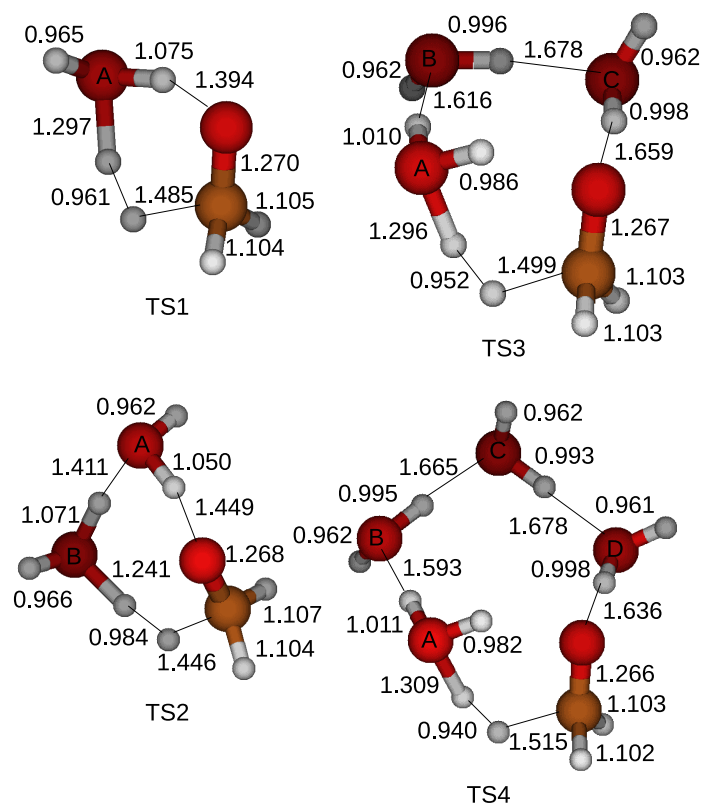


Figure 4. Optimized structures of the transition states for the oxidation of a CH_3OH when a CH_3OH and H_2O molecules form a ring structure. Four labels (A, B, C, D) are affixed to oxygen atoms of H_2O molecules to distinguish. We apply the Gaussian 4 method and optimize the transition states. H_2O molecules assist the oxidation of a CH_3OH and up to four H_2O molecules are included in the simulations. TS_n stands for Transition States when the oxidation of a CH_3OH is catalyzed by n H_2O molecules in a ring structure.

We adopt the transition states and carry out the IRC calculations with the 6-311+G(3df, 2p) basis set to follow the minimum energy reaction pathway. Reactant and product compounds are located at local minimums. We further apply the Gaussian 4 method to obtain the optimized structures of the reactant and product compounds. The optimized structures of the reactant compounds and the product compounds are shown in Figures 5 and 6. A hydrogen bond is formed when an oxygen atom faces a neighbor hydrogen atom. A hydrogen bond network contains a hydroxyl of a CH_3OH as shown in Figure 5. The total energy of a reactant compound is reduced by the formed hydrogen bonds inside the reactant compound.

Figure 6 shows the structures of the product compounds, an HCHO , an H_2 , and H_2O molecules, when a CH_3OH and H_2O molecules form a ring structure in a transition state. An HCHO in a product compound has approximately the same structure with that shown in Figure 1. The hydrogen bonds stretch the CO bond weakly by a factor of 1.01. We confirm that the final products yielded from the oxidation of a CH_3OH are an HCHO and an H_2 . The total energy of a product compound is also reduced due to the formed hydrogen bonds inside the product compound. A ring structure of a supermolecule is reconstructed after the oxidation.

We calculate the energy barrier from the difference of the electronic energies corrected by the zero point energy between a transition state and a reactant compound. We find the electronic energy and the zero point energy with the Gaussian 4 method.

The energy barrier for the oxidation of a CH_3OH is shown in Figure 7 and Table 1. The free energy differences between a reactant compound and a transition state at 298.15 K are also displayed in Table 1. The energy barrier for the oxidation of a CH_3OH decreases from 90.9 kcal/mol to 65.2 kcal/mol when a single H_2O molecule is included in a simulation. This indicates the catalytic role of a H_2O molecule during the oxidation of a CH_3OH . The energy barrier decreases further when more H_2O molecules are introduced in the simulation and has a minimum value of 61.2 kcal/mol when three H_2O molecules are included in the simulation.

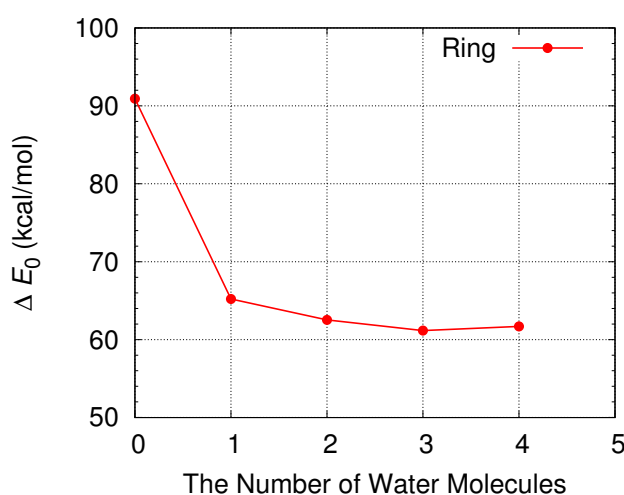


Figure 7. The energy barrier for the oxidation of a CH_3OH in water with and without the catalyst of H_2O molecules when a CH_3OH and H_2O molecules form a ring structure. The energy barrier is calculated from the difference of the electronic energies corrected by the zero point energy between a transition state and a reactant compound.

Table 1. The energy barriers (kcal/mol) as well as the free energy differences (kcal/mol) at 298.15 K between a reactant compound and a transition state for the oxidation of a CH_3OH in water without and with the catalyst of H_2O molecules. We consider the oxidation processes catalyzed by H_2O molecules in the following two arrangements: (1) a CH_3OH and H_2O molecules form a ring structure, and (2) a CH_3OH is bonded to a cluster of H_2O molecules by hydrogen bonds.

Number of H_2O Molecules	$n = 0$	$n = 1$	$n = 2$	$n = 3$	$n = 4$	$n = 5$
ΔE_0 (Ring)	90.9	65.2	62.5	61.2	61.7	
ΔE_0 (Cluster)					62.5	58.5
ΔG (Ring)	91.0	68.2	63.9	63.2	64.0	
ΔG (Cluster)					65.2	58.6

A cluster of H_2O molecules was shown to play an active role as catalyst in the decomposition of formic acid and methanediol [7,8]. A hydrogen bond in liquid water forms when a proton of an H_2O molecule faces an oxygen atom of a neighbor H_2O molecule. It is natural to consider that H_2O molecules in liquid water develop a network of hydrogen bonds and frequently organize a cluster of H_2O molecules. Experimental studies with the far-infrared vibrational-rotational-tunneling spectroscopy confirmed small clusters consisted of 2, 3, 4, and 5 H_2O molecules [23–26]. A cluster of H_2O molecules has a cyclic network of hydrogen bonds. The intermolecular distance between

H₂O molecules decreases by the cooperative many body interactions in a cluster of H₂O molecules. A proton is efficiently transferred between H₂O molecules within a cluster of H₂O molecules.

A cluster of H₂O molecules is expected to reduce the energy barrier in the oxidation of CH₃OH as well. We include clusters with 4 and 5 H₂O molecules in the simulations and examine the catalytic role of a cluster of H₂O molecules in the oxidation of CH₃OH. Figure 8 shows the optimized structures of the reactant compounds, the transition states, and the product compounds for the oxidation of a CH₃OH catalyzed by a cluster of H₂O molecules. A CH₃OH uses two H₂O molecules with the labels A and B within a cluster of H₂O molecules to transfer a proton of the hydroxyl of a CH₃OH, while the rest of H₂O molecules in the cluster supports the two H₂O molecules with hydrogen bonds. The oxidation process starts when a proton of an H₂O molecule with the label A is transferred to an H₂O molecule with the label B within a cluster of H₂O molecules. An H₂O molecule with the label A supplements the lost proton with a proton from a hydroxyl of a CH₃OH. A transition state is formed when a proton is detached from a methyl of a CH₃OH. An H₂O molecule with the label B loses an extra proton, which is combined with a free proton detached from the methyl of a CH₃OH, yielding an H₂. Clusters of four and five H₂O molecules are recovered in product compounds and might catalyze another oxidation of a CH₃OH.

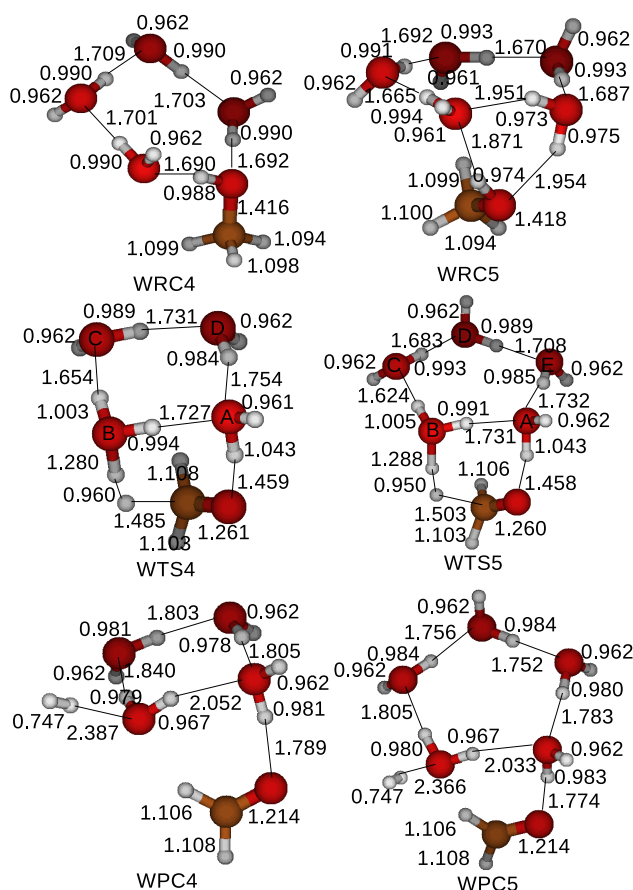


Figure 8. Optimized structures of a reactant compound, a transition state, and a product compound when a cluster of H₂O molecules catalyzes the oxidation of a CH₃OH. The Gaussian 4 method is applied to locate and optimize the reactant compounds, transition states, and the product compounds. We consider clusters of 4 and 5 H₂O molecules in the simulations. Labels (A, B, C, D, E) are affixed to oxygen atoms of H₂O molecules in transition states to distinguish. WRC_n, WTS_n, and WPC_n stand for a Reactant Compound, a Transition State, and a Product Compound for the oxidation of a CH₃OH catalyzed by a cluster with *n* H₂O molecules.

The energy barrier for the oxidation of a CH_3OH is shown in Figure 9 when a cluster of H_2O molecules catalyzes the oxidation. For comparison the energy barrier is also shown when a CH_3OH and H_2O molecules form a ring structure. The energy barrier for the oxidation of a CH_3OH catalyzed by a cluster of four H_2O molecules is nearly the same with that for the oxidation of a CH_3OH by four H_2O molecules in a ring structure. The energy barrier is reduced when a cluster of five H_2O molecules catalyzes the oxidation. We obtain the lowest energy barrier of 58.5 kcal/mol when a cluster with five H_2O molecules is included in the simulation. The energy barrier is about 3 kcal/mol lower than the lowest energy barrier obtained when a ring structure is formed by a CH_3OH and H_2O molecules.

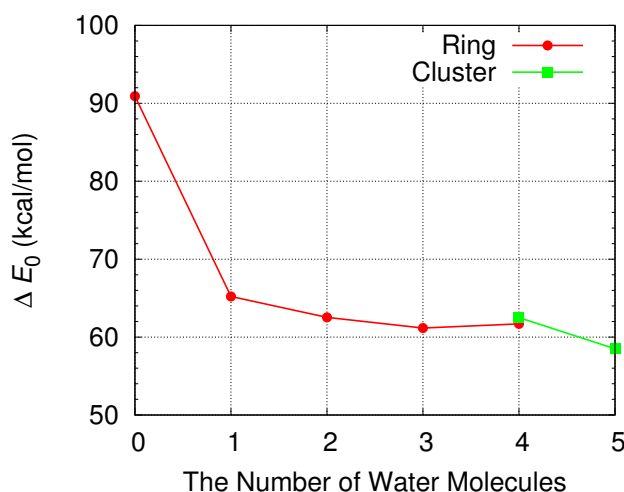


Figure 9. The energy barrier for the oxidation of a CH_3OH in water when H_2O molecules in a ring structure and a cluster of H_2O molecules catalyze the oxidation of a CH_3OH . The energy barrier is calculated from the difference of the electronic energies corrected by the zero point energy between a transition state and a reactant compound.

In order to describe the entire decomposition processes of CH_3OH , we need to consider the sequence of decompositions after HCHO : (1) from HCHO to $\text{CH}_2(\text{OH})_2$, (2) from $\text{CH}_2(\text{OH})_2$ to HCOOH , and (3) from HCOOH to CO or CO_2 . We performed the ONIOM(QM/MM) simulations [27–30] and revealed that HCHO is hydrated to become $\text{CH}_2(\text{OH})_2$ with the low energy barrier of about 20 kcal/mol [9]. It is possible to consider the decomposition path from HCHO to CO , but it was shown that the energy barrier for this path becomes 61 kcal/mol and is higher than the energy barrier of 49 kcal/mol for the decomposition of $\text{CH}_2(\text{OH})_2$ into HCOOH [10]. We further examined the decomposition of HCOOH and calculated the energy barriers for the decomposition of HCOOH into CO or CO_2 . Both energy barriers are shown to be lower than 40 kcal/mol [7]. The energy barriers for the decomposition of HCHO into CO or CO_2 are much lower than the energy barrier of 58.5 kcal/mol to decompose CH_3OH into HCHO . The rate constant for the decomposition of CH_3OH into CO or CO_2 is mainly determined by the rate constant to oxidize CH_3OH into HCHO . We calculate the rate constant with Equation (3) and compare it with the decomposition rate of CH_3OH determined by laboratory experiments.

Figure 10 shows the calculated rate constants for the oxidation of a CH_3OH catalyzed by up to five H_2O molecules as a function of the temperature. The rate constant for the oxidation of a CH_3OH increases with an increase in the temperature regardless of the number of H_2O molecules included in the simulations. When H_2O molecules and a CH_3OH form a ring structure in a simulation, the highest rate constant is obtained when two H_2O molecules catalyzes the oxidation of a CH_3OH . The rate constant is further enhanced by the catalyst of a cluster of five H_2O molecules by a factor of 94.

Figure 10 also shows that the rate constants for the oxidation of CH_3OH determined by laboratory experiments. The oxidation of CH_3OH was examined using a Ni alloy reactor in experiments [3,6,31].

The rate constants determined by Hack et al. [3] is much larger than that calculated in the present study, indicating the catalytic role of the Ni alloy surface of a reactor. It was confirmed that the reactor surface acts as catalyst for the oxidation of CH_3OH and increases the rate constant considerably. The oxidation rate is dependent on the surface condition of a reactor and is reduced by a factor of 1000 when the reactor surface is treated with $\text{HNO}_3/\text{H}_2\text{O}_2$ before an experiment [3]. Hirsh and Franck [6] and Bennekom et al. [31] also used Ni alloy reactors to study the oxidation of CH_3OH , however, their reactors have a surface to volume ratio smaller than that used by Hack et al. (2005), suggesting the weaker catalytic role of the surface of the reactor. It is shown in Figure 10 that the rate constants given by Hirsh and Franck (1993) and Bennekom et al. (2011) are much slower than that given by Hack et al. (2005). On the other hand, DiLeo and Savage [1] performed experiments for the oxidation of CH_3OH in a sealed quartz tube to determine the oxidation rate of CH_3OH without any catalytic effect of a reactor surface. The slowest oxidation of CH_3OH was discovered due to the lack of catalytic effect of a reactor wall as shown in Figure 10, even though only a single data point was given.

The calculated rate constant is smaller than that given by DiLeo and Savage (2006) when we only consider the catalyst of H_2O molecules in a ring structure with a CH_3OH . The oxidation of CH_3OH catalyzed by a cluster of five H_2O molecules is required to be included to explain the measured oxidation rate of DiLeo and Savage (2006). The oxidation of CH_3OH determined by the experiment is well explained if we consider three percent of CH_3OH molecules are decomposed with the help of the catalyst of a cluster of five H_2O molecules. The catalytic effect of Ni metal surface needs to be considered when we explain the oxidation rate of CH_3OH determined by Hack et al. (2005) in a Ni alloy reactor.

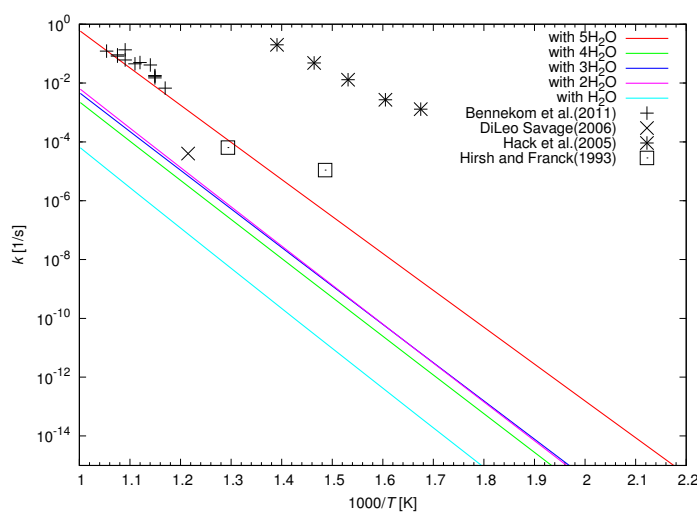


Figure 10. Rate constants for the oxidation of a CH_3OH measured in a laboratory [1,3,6,31] as well as that calculated in this study. The rate constant is calculated when the oxidation is catalyzed by up to four H_2O molecules in a ring structure or by a cluster of five H_2O molecules.

3. Computational Method

A simple model for the oxidation process of a CH_3OH in water is used at the present study. We consider the molecular oxidation of a CH_3OH , the product of which are a formaldehyde, HCHO , and a hydrogen molecule, H_2 , given by



even though a CH_3OH is expected to decompose into radicals in the gas phase at the high temperature. The interaction of a CH_3OH with another CH_3OH is not considered in this study. Single carbon compounds such as methane might be formed in an experiment, however we do not consider any

reactions involving single carbon compounds other than a CH₃OH. A CH₃OH decomposes into an HCHO and an H₂ and interacts with nothing but some H₂O molecules when H₂O molecules act as catalyst for the oxidation of a CH₃OH.

The previous studies showed a crucial role of H₂O molecules to lower the energy barrier for the oxidation of formic acid and methanediol in water [7,8]. We perform molecular dynamical simulations with the Amber 16 [32] and find the distribution of H₂O molecules around a CH₃OH even though a molecular dynamical simulation is not useful to study the formation and breaking of molecular bonds. A CH₃OH and H₂O molecules are located in a box and interact with each other. The temperature and the pressure of a box are regulated to be constant values, $T = 300$ K and 1 atm. A three point model of TIP3P is used to describe a H₂O molecule [33]. We adopt the periodic boundary conditions with the particle mesh Ewald method to take into account the electric forces of H₂O molecules outside of the box. The positions of the CH₃OH and H₂O molecules are recorded every 0.1 ps. We obtain the number density distribution of the H₂O molecules around the CH₃OH by averaging 1000 coordinate data.

A proton is transferred from a reactant to a neighbor H₂O molecule to promote the oxidation process efficiently. We need to include some H₂O molecules in quantum chemical simulations to follow the formation and breaking processes of bonds between a proton and an H₂O molecule. We adopt the Gaussian 16 software [34] to perform quantum simulations for the oxidation of a CH₃OH in water. We deal with a supermolecule consisting of a CH₃OH and H₂O molecules when we examine the catalytic role of H₂O molecules in the oxidation of CH₃OH. We use the Gaussian 4 method and optimize the structure of a supermolecule because the Gaussian 4 method is reliable to calculate the enthalpy of formation [35]. The electronic energies as well as the vibrational frequencies at 0 K of a reactant compound, a transition state, and a product compound are calculated using the optimized structures of a supermolecule. We add thermal correction as a result of translation, rotation, and vibration of atomic nuclei to the electronic energy and obtain the total energy of a supermolecule. The energy barrier, ΔE_0 , for the oxidation of a CH₃OH is given by the difference of the electronic energies corrected by the zero point energy between a transition state and a reactant compound.

Transition state theory expresses the oxidation rate of a CH₃OH as

$$k = \Gamma^* \frac{k_B T}{h} \frac{q_{\ddagger}}{q_{rc}} \exp(-\Delta E_0/k_B T), \quad (3)$$

where Γ^* is an enhanced factor due to the tunneling of a proton through an energy barrier, q_{\ddagger} and q_{rc} are the partition functions of a transition state and a reactant compound, and h , k_B , and T , are the Planck constant, the Boltzmann constant, and the temperature, respectively. We calculate the enhanced factor due to the tunneling following our previous study [7] by approximating the energy barrier with the unsymmetrical Eckart potential. We carry out the IRC calculation and follow the minimum energy pathway to find a reactant compound and a product compound. The discovered reactant compound and product compound are further optimized with the Gaussian 4 method.

The partition function is calculated from the product of the partition functions due to translation, rotation, and vibration. Furthermore, the oxidation rate relies only on the partition functions of the rotation and the vibration because both a reactant compound and a transition state have nearly the same partition function for the translation. The rotational partition function is calculated from

$$q_r = \sqrt{\frac{\pi T^3}{\Theta_x \Theta_y \Theta_z}}, \quad (4)$$

where Θ_x , Θ_y and Θ_z are the rotational temperatures. The vibrational partition function of a supermolecule is given by

$$q_v = \prod_i^{3N-6} \frac{1}{1 - \exp(-h\nu_i/k_B T)}, \quad (5)$$

where ν_i is the frequency of the i -th vibrational mode and N is the total number of atoms contained in the supermolecule. The rotational temperatures and the vibrational frequencies are shown in the output file of the Gaussian 4 and used to obtain the partition functions of a transition state and a reactant compound with Equations (4) and (5).

4. Conclusions

We have examined the catalytic role of H₂O molecules in the oxidation of CH₃OH in water. We performed quantum chemical simulations with the Gaussian 4 method. The optimized structure of a CH₃OH agrees well with that determined by experimental studies, guaranteeing the capability of the Gaussian 4 method. It was shown that H₂O molecules near a CH₃OH serve as effective catalyst in the oxidation of a CH₃OH. The energy barrier for the oxidation of a CH₃OH is reduced by 25.7 kcal/mol when a single H₂O molecule is included in the simulation and decreases further if more H₂O molecules get involved in the oxidation of a CH₃OH. H₂O molecules help to transfer a proton efficiently from a hydroxyl of a CH₃OH to the proximity of the CH-bond in the CH₃OH without significant change of the structure. The oxidation of a CH₃OH is completed after the two protons combine to form an H₂.

A number of hydrogen bonds frequently arise in liquid water. Some H₂O molecules are joined together by a chain of hydrogen bonds. A cluster of H₂O molecules is formed by an enclosed chain of hydrogen bonds. A cluster of H₂O molecules is included in the simulation for the oxidation of a CH₃OH. The energy barrier for the oxidation of a CH₃OH is reduced further by a cluster of H₂O molecules because a proton is transferred with less energy between H₂O molecules within a cluster of H₂O molecules. The minimum energy barrier is obtained when a cluster of five H₂O molecules catalyzes the oxidation of a CH₃OH.

We applied transition state theory to calculate the oxidation rate of a CH₃OH considering the tunneling effect of a proton. The tunneling effect slightly increases the oxidation rate at the low temperature. The oxidation rate of a CH₃OH increases with the increasing temperature. The calculated oxidation rate increases with the number of H₂O molecules and has the maximum when a cluster of five H₂O molecules catalyzes the oxidation of a CH₃OH. The rapid oxidation of CH₃OH was measured when CH₃OH is decomposed in a Ni alloy reactor. The oxidation becomes slow when CH₃OH is decomposed without any catalyst in a sealed quartz reactor. The oxidation rate of CH₃OH in water without catalyst is well explained if we consider that three percent of CH₃OH molecules are decomposed with the catalyst of a cluster of five H₂O molecules, while the oxidation of the rest of the CH₃OH molecules is catalyzed by two H₂O molecules in a ring structure.

Acknowledgments: Computations were performed in Research Center for Computational Science, Okazaki, Japan.

Conflicts of Interest: The authors declare no conflict of interest.

References

1. DiLeo, G.J.; Savage, P.E. Catalysis during Methanol Gasification in Supercritical Water. *J. Supercrit. Fluids* **2006**, *39*, 228–232.
2. Dombrowsky, C.; Hoffmann, A.; Klatt, M.; Wagner, H.G. An Investigation of the Methanol Decomposition Behind Incident Shock Waves. *Ber. Bunsenges. Phys. Chem.* **1991**, *95*, 1685.
3. Hack, W.; Masten, D.A.; Buelow, S.J. Methanol and Ethanol Decomposition in Supercritical Water. *Z. Phys. Chem.* **2005**, *219*, 367–378.
4. Boukis, N.; Diem, V.; Habicht, W.; Dinjus, E. Methanol Reforming in Supercritical Water. *Ind. Eng. Chem. Res.* **2003**, *42*, 728–735.
5. Tester, J.W.; Webley, P.A.; Holgate, H.R. Revised Global Kinetic Measurements of Methanol Oxidation in Supercritical Water. *Ind. Eng. Chem. Res.* **1993**, *32*, 236–239.
6. Hirth, T.; Franck, E.U. Oxidation and Hydrothermolysis of Hydrocarbons in Supercritical Water at High Pressures. *Ber. Bunsenges. Phys. Chem.* **1993**, *97*, 1091.

7. Inaba, S. Theoretical Study of Water Cluster Catalyzed Decomposition of Formic Acid. *J. Phys. Chem. A* **2014**, *118*, 3026–3028.
8. Inaba, S. Theoretical Study of Decomposition of Methanediol in Aqueous Solution. *J. Phys. Chem. A* **2015**, *119*, 5816–5825.
9. Inaba, S.; Sameera, W.M.C. Dehydration of Methanediol in Aqueous Solution: An ONIOM(QM/MM) Study. *J. Phys. Chem. A* **2016**, *119*, 5816–5825.
10. Inaba, S. Primary Formation Path of Formaldehyde in Hydrothermal Vents. *Orig. Life Evol. Biosph.* **2018**, *48*, 1–22.
11. Hartnig, C.; Spohr, E. The Role of Water in the Initial Steps of Methanol Oxidation on Pt(1 1 1). *Chem. Phys.* **2005**, *319*, 185–191.
12. Becke, A.D. Density-Functional-Exchange-Energy Approximation with Correct Asymptotic Behavior. *Phys. Rev. A Opt. Phys.* **1988**, *38*, 3098–3100.
13. Lee, C.; Yang, W.; Parr, R.G. Development of The Colle-Salvetti Correlation-Energy Formula into A Functional of The Electron Density. *Phys. Rev. B Condens. Matter Mater. Phys.* **1988**, *37*, 785–789.
14. Miehlich, B.; Savin, A.; Stoll, H.; Preuss, H. Results Obtained with The Correlation Energy Density Functionals of Becke and Lee, Yang and Parr. *Chem. Phys. Lett.* **1989**, *157*, 200–206.
15. Ditchfield, R.; Hehre, W.J.; Pople, J.A. Self-Consistent Molecular-Orbital Methods. IX. An Extended Gaussian-Type Basis for Molecular-Orbital Studies of Organic Molecules. *J. Chem. Phys.* **1971**, *54*, 724–728.
16. Hehre, W.J.; Ditchfield, R.; Pople, J.A. Self-Consistent Molecular-Orbital Methods. XII. Further Extensions of Gaussian-Type Basis Sets for Uses in Molecular Orbital Studies of Organic Molecules. *J. Chem. Phys.* **1972**, *56*, 2257–2261.
17. Clark, T.; Chandrasekhar, J.; Spitznagel, G.W.; von Ragué Schleyer, P. Efficient Diffuse Function-Augmented Basis Sets for Anion Calculations. III. The 3-21+G Basis Set for First-Row Elements, Li-F. *J. Comp. Chem.* **1983**, *4*, 294–301.
18. Frisch, M.J.; Pople, J.A.; Binkley, J.S. Self-Consistent Molecular Orbital Methods 25. Supplementary Functions for Gaussian Basis Sets. *J. Chem. Phys.* **1984**, *80*, 3265–3269.
19. Schaftenaar, G.; Noordik, J.H. Molden: A Pre- and Post-Processing Program for Molecular and Electronic Structures. *J. Comput.-Aided Mol. Des.* **2000**, *14*, 123–134.
20. Florián, J.; Leszczynski, J.; Johnson, B.G.; Goodman, L. Coupled-Cluster and Density Functional Calculations of The Molecular Structure, Infrared Spectra, Raman Spectra, and Harmonic Force Constants for Methanol. *Mol. Phys.* **1997**, *91*, 439–447.
21. Yamada, K.; Nakagawa, T.; Kuchitsu, K.; Morino, Y. Band Contour Analysis of the ν_1 and ν_5 Fundamentals of Formaldehyde. *J. Mol. Spectrosc.* **1971**, *38*, 70–83.
22. Johnson, R.D., III. *NIST Computational Chemistry Comparison and Benchmark Database*; NIST Standard Reference Database: Gaithersburg, MD, USA, 2016.
23. Pugliano, N.; Saykally, R.J. Measurement of the ν_8 Intermolecular Vibration of $(D_2O_2)_2$ by Tunable Far Infrared Laser Spectroscopy. *J. Chem. Phys.* **1992**, *96*, 1832–1839.
24. Pugliano, N.; Saykally, R.J. Measurement of Quantum Tunneling Between Chiral Isomers of the Cyclic Water Trimer. *Science* **1992**, *257*, 1937–1940.
25. Cruzan, J.D.; Braly, L.B.; Liu, K.; Brown, M.G.; Loeser, J.G.; Saykally, R.J. Quantifying Hydrogen Bond Cooperativity in Water: VRT Spectroscopy of the Water Tetramer. *Science* **1996**, *271*, 59–62.
26. Liu, K.; Brown, M.G.; Cruzan, J.D.; Saykally, R.J. Vibration-Rotation Tunneling Spectra of the Water Pentamer: Structure and Dynamics. *Science* **1996**, *271*, 62–64.
27. Maseras, F.; Morokuma, K. IMOMM: A New Integrated Ab Initio + Molecular Mechanics Geometry Optimization Scheme of Equilibrium Structures and Transition States. *J. Comput. Chem.* **1995**, *16*, 1170–1179.
28. Humbel, S.; Sieber, S.; Morokuma, K. The IMOMO Method: Integration of Different Levels of Molecular Orbital Approximations for Geometry Optimization of Large Systems: Test for *n*-butane Conformation and S_N2 Reaction: $RCI + Cl^-$. *J. Chem. Phys.* **1996**, *105*, 1959–1967.
29. Dapprich, S.; Komáromi, I.; Byun, K.S.; Morokuma, K.; Frisch, M.J. A New ONIOM Implementation in Gaussian98. Part I. The Calculation of Energies, Gradients, Vibrational Frequencies and Electric Field Derivatives. *J. Mol. Struct.* **1999**, *461–462*, 1–21.
30. Chung, L.W.; Sameera, W.M.C.; Ramozzi, R.; Page, A.J.; Hatanaka, M.; Petroya, G.P.; Harris, T.V.; Li, X.; Ke, Z.; Liu, F.; et al. The ONIOM Method and Its Applications. *Chem. Rev.* **2015**, *115*, 5678–5796.

31. Van Bennekom, J.G.; Venderbosch, R.H.; Assink, D.; Heeres, H.J. Reforming of Methanol and Glycerol in Supercritical Water. *J. Supercrit. Fluids* **2011**, *58*, 99–113.
32. Case, D.A.; Cerutti, D.S., Cheatham, T.E., III; Darden, T.A.; Duke, R.E.; Giese, T.J.; Gohlke, H.; Goetz, A.W.; Greene, D.; Homeyer, N.; et al. *AMBER 17*; University of California: San Francisco, CA, USA, 2017.
33. Jorgensen, W.L.; Chandrasekhar, J.; Madura, J.D.; Impey, R.W.; Klein, M.L. Comparison of Simple Potential Functions for Simulating Liquid Water. *J. Phys. Chem.* **1983**, *2*, 926–935.
34. Frisch, M.J.; Trucks, G.W.; Schlegel, H.B.; Scuseria, G.E.; Robb, M.A.; Cheeseman, J.R.; Scalmani, G.; Barone, V.; Petersson, G.A.; Nakatsuji, H.; et al. *Gaussian 16, Revision A.03*; Gaussian, Inc.: Wallingford, CT, USA, 2016.
35. Curtiss, L.; Redfern, P.; Raghavachari, K. Gaussian-4 Theory. *J. Chem. Phys.* **2007**, *126*, 084108.



© 2018 by the author. Licensee MDPI, Basel, Switzerland. This article is an open access article distributed under the terms and conditions of the Creative Commons Attribution (CC BY) license (<http://creativecommons.org/licenses/by/4.0/>).